CHARMONIUM PRODUCTION IN Pb–Pb COLLISIONS WITH ALICE*

Jon-Are Sætre

for the ALICE Collaboration

University of Bergen, Norway
jon-are.saetre@cern.ch

Received 15 August 2022, accepted 24 August 2022, published online 14 December 2022

Charmonium production is a direct probe of the quark–gluon plasma (QGP), a deconfined state of nuclear matter formed in heavy-ion collisions. For J/ψ, a bound state of $c\bar{c}$ quarks, its (re-)generation within the QGP or at the phase boundary, is found to be the dominant production mechanism at low transverse momentum ($p_{\rm T}$) and in central Pb–Pb collisions at the LHC energies. The relative production of the $\psi(2S)$ excited state with respect to the J/ψ is one possible discriminator between the two different regeneration scenarios. In addition, the non-prompt component of J/ψ production from b-hadron decays allows one to access the interaction of beauty quarks inside the QGP down to low $p_{\rm T}$. In these proceedings, we present, for the first time, results on the $\psi(2S)$-to-J/ψ double ratio in Pb–Pb collisions at forward rapidity and $\sqrt{s_{NN}} = 5.02$ TeV with respect to a new pp reference with an improved precision compared to the earlier publications. The combined Run 2 data set of ALICE allows the extraction of a signficant $\psi(2S)$ signal in central Pb–Pb collisions at forward rapidity down to zero transverse momentum. The $\psi(2S)$ nuclear modfication factor R_{AA} as a function of $p_{\rm T}$ and centrality will also be shown, as well as the inclusive J/ψ R_{AA} at forward rapidity. At midrapidity, the inclusive, prompt and non-prompt J/ψ R_{AA} as a function of centrality and $p_{\rm T}$ will be presented, based on the full Run 2 statistics. The extraction of the non-prompt J/ψ fraction extends other LHC measurements down to very low $p_{\rm T}$ and its precision is improved signficantly compared to previous ALICE publications. Results will be compared with available theoretical model calculations.

DOI:10.5506/APhysPolBSupp.16.1-A115

1. Introduction

Charmonia are excellent probes of the quark–gluon plasma (QGP) as they are produced in the early stage of the heavy-ion collision, so they can

* Presented at the 29th International Conference on Ultrarelativistic Nucleus–Nucleus Collisions: Quark Matter 2022, Kraków, Poland, 4–10 April, 2022.

experience the full collision history. Looking at the J/ψ and one of its excited states, the $\psi(2S)$, the latter is expected to be more suppressed in the QGP compared to the former. The reason for this is the sequential dissociation of the charmonium states in the medium according to their binding energies [1]. Due to the high $c\bar{c}$ pair production cross section at the LHC energies, charmonia can also be produced via regeneration at either the phase boundary or during the QGP phase. In particular, in the statistical hadronisation scenario [2, 3], the relative abundances of all hadrons, including charmonium states, are determined at chemical freezeout according to thermal weights. In the transport models, charmonia are continuously produced and broken up during their propagation through the QGP [4–6]. The ratio of the $\psi(2S)$ and J/ψ production yields represents a great tool to disentangle between the two regeneration scenarios due to the partial cancellation of both theoretical and experimental uncertainties. In particular, the $\psi(2S)$-to-J/ψ ratio is weakly dependent on the total $c\bar{c}$ production cross section used as inputs to the theoretical models, and which still suffer from large experimental uncertainties.

A sizeable fraction of charmonia comes from beauty hadron decays, granting access to open heavy-flavor production. Heavy quarks, charm and beauty, are produced early in heavy-ion collisions via hard parton–parton scatterings. For high-p_{T} quarks, their main manifestation of the interactions with the QGP is energy loss, which can occur via collisional processes and gluon radiation [7, 8]. In addition, the dead cone effect [9] predicts gluon radiation to be suppressed for angles $\theta < m/E$, where m and E are the quark mass and energy. Collisional energy loss is predicted to depend on the quark mass and to be smaller for heavy quarks [10].

The ALICE detector [11] has unique capabilities at the LHC for measuring inclusive charmonia down to zero transverse momentum. Measurements are carried out at both central and forward rapidity, in the dielectron and dimuon decay channel, respectively. At midrapidity, one can also disentangle the prompt J/ψ contribution from the one originating from beauty hadrons decays (non-prompt J/ψ), down to 1.5 GeV/c in Pb–Pb collisions. At midrapidity, the main detectors employed in the analysis are the time projection chamber (TPC) and the inner tracking system (ITS). While the TPC is used for tracking and particle identification, the ITS is used for tracking and vertex reconstruction. In particular, the two innermost layers of the ITS, which are made of silicon pixel detectors, enable the disentanglement of prompt and non-prompt J/ψ. At forward rapidity, the muon spectrometer is used for triggering and tracking of the muons. The V0 detectors, which consist of two scintillator arrays covering the forward $(2.8 < \eta < 5.1)$ and backward $(-3.7 < \eta < -1.7)$ pseudorapidity regions, are used for centrality determination, triggering and background rejection.

2. Charmonium results: selected highlights

Prompt and non-prompt J/ψ R_{AA}

The nuclear modification factor (R_{AA}) is defined as the ratio of the production yield in nucleus–nucleus collisions to the production cross section in proton–proton collisions scaled by the average nuclear overlap function [22]. Thanks to the determination of the non-prompt J/ψ fraction, it is possible to determine both prompt and non-prompt J/ψ R_{AA}. The following measurements are using the full Run 2 statistics. As shown in the top panel of Fig. 1, the preliminary measurement of the prompt J/ψ R_{AA} performed by ALICE at midrapidity exhibits a rising trend towards low p_{T}, reaching values above unity for $p_{\mathrm{T}} < 3$ GeV$/c$. For $p_{\mathrm{T}} < 5$ GeV$/c$, the prompt J/ψ R_{AA} shows good agreement with predictions from SHMc [15], the statistical hadronization model extended to the charm sector, which considers

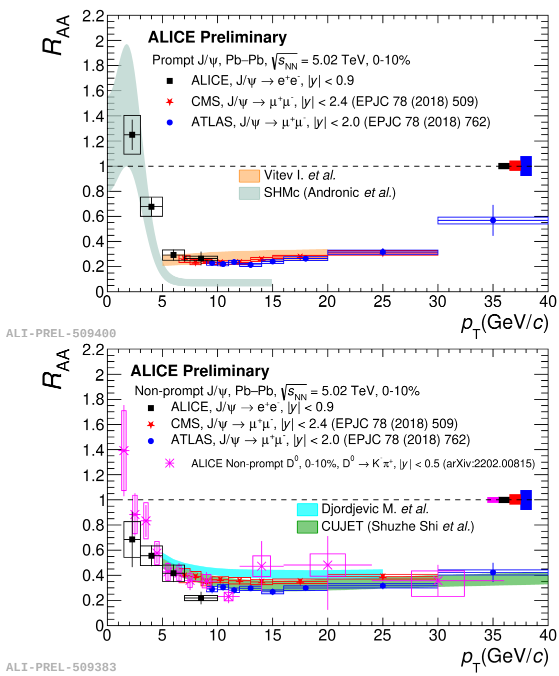

Fig. 1. R_{AA} as a function of p_{T} measured at midrapidity for the prompt (top panel) and non-prompt (bottom panel) J/ψ in Pb–Pb collisions at $\sqrt{s_{NN}} = 5.02$ TeV. Measurements performed by the CMS [12] and ATLAS [13] collaborations, which are available at higher p_{T}, are also shown. Non-prompt J/ψ are also compared to non-prompt D^0 R_{AA} measurements from ALICE [14]. Theoretical model predictions for both prompt J/ψ (SHMc [15] and Vitev *et al.* [16, 17]) and non-prompt J/ψ (CUJET model [18, 19] and Djordjevic *et al.* [20, 21]) are also shown.

a regeneration mechanism for both charmonia and open (multiple) charm hadrons. The model by Vitev *et al.* [16, 17], which combines collisional dissociation of quarkonia and the screening of the attractive potential inside the QGP, describes the ALICE results within uncertainties, as well as the CMS and ATLAS measurements at high p_{T}. For both non-prompt D^0 and non-prompt J/ψ, shown in the bottom panel of Fig. 1, there is a strong decrease of the R_{AA} at high p_{T}, while it shows an increasing trend moving towards lower p_{T}, hinting at beauty quark production being pushed towards lower p_{T}, as expected due to heavy quark number conservation. Both the CUJET model [18, 19] and the model by Djordjevic *et al.* [20, 21], implementing radiative and collisional energy loss mechanisms, are consistent with the data within uncertainties.

Figure 2 shows the prompt and non-prompt J/ψ R_{AA} as a function of the average number of nucleons participating in the collision. They are comparable in all centrality intervals, except for the most central collisions, where the non-prompt J/ψ R_{AA} is significantly below unity. However, within uncertainties, there is not much variation of the non-prompt J/ψ R_{AA} with centrality. Conversely, the prompt J/ψ the R_{AA} rises in the most central collisions, and this is expected according to the regeneration scenario.

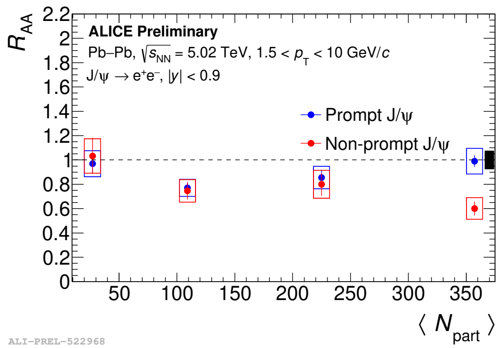

Fig. 2. R_{AA} as a function of $\langle N_{\text{part}} \rangle$ for the prompt and non-prompt J/ψ measured at midrapidity in Pb–Pb collisions at $\sqrt{s_{NN}} = 5.02$ TeV.

$\psi(2S)$ R_{AA} and $\psi(2S)$-to-J/ψ ratio

Inclusive $\psi(2S)$ and J/ψ R_{AA} results at forward rapidity are shown in Fig. 3 (left) as a function of p_{T}. The TAMU transport model [5], which includes charmonium regeneration through the QGP, is able to reproduce both charmonium state measurements as a function of $\langle N_{\text{part}} \rangle$ (not shown) and p_{T} (see Fig. 3 (left)). In particular, the rising trend of the R_{AA} towards low p_{T} hints at regeneration for both $\psi(2S)$ and J/ψ. The plot on the right side of Fig. 3 shows the centrality dependence of the $\psi(2S)$-to-J/ψ ratio (top panel) and the double ratio to pp collisions (bottom panel) measured in Pb–Pb at $\sqrt{s_{NN}} = 5.02$ TeV. A suppression effect of about 40% with respect to *pp* can be seen in the double ratio. TAMU reproduces nicely the $\psi(2S)$-to-J/ψ ratio, while SHMc underestimates the data in the most central collisions. NA50 results in Pb–Pb collisions at $\sqrt{s_{NN}} = 17.3$ GeV [23] are shown for comparison. The $\psi(2S)$-to-J/ψ ratio and the double ratio at SPS energy exhibit a stronger centrality dependence, and smaller values in central events with respect to ALICE data.

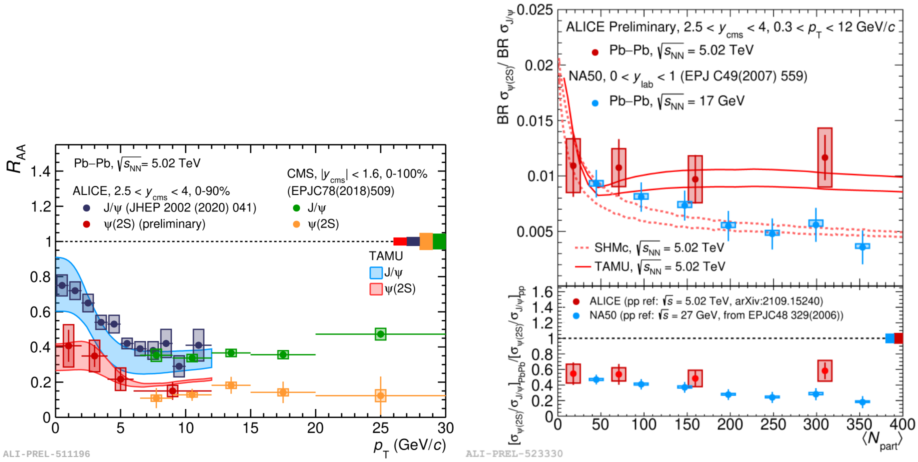

Fig. 3. Left: Inclusive J/ψ and $\psi(2S)$ R_{AA} measured at forward rapidity as a function of p_{T} in the centrality range of 0–90% in Pb–Pb collisions at $\sqrt{s_{NN}} = 5.02$ TeV. The TAMU predictions [5] are shown for comparison. CMS measurements [12] at midrapidity in the centrality range of 0–100% are also shown at high p_{T}. Right: $\psi(2S)$-to-J/ψ ratio measured by ALICE at forward rapidity in Pb–Pb collisions at $\sqrt{s_{NN}} = 5.02$ TeV as a function of $\langle N_{\mathrm{part}} \rangle$. The TAMU [5] and SHMc [15] model predictions at LHC energies are shown in addition to SPS NA50 measurements [23] at $\sqrt{s_{NN}} = 17.3$ GeV. In the lower panel, the $\psi(2S)$-to-J/ψ ratio in Pb–Pb collisions is normalized to the corresponding value in *pp* collisions (double ratio).

3. Conclusions

Measurements of the nuclear modification factor of inclusive $\psi(2S)$ and J/ψ at forward rapidity as well as prompt J/ψ at midrapidity in Pb–Pb collisions at $\sqrt{s_{NN}} = 5.02$ TeV, indicate a strong contribution from regeneration in the low-p_{T} region and suppression at high p_{T}. The statistical hadronisation model describes well within uncertainties the prompt J/ψ R_{AA} at midrapidity, while the transport model shows a good agreement with the $\psi(2S)$ and J/ψ R_{AA} measurements at forward rapidity. The TAMU model describes the $\psi(2S)$-to-J/ψ ratio, while SHMc underestimates it in most central collisions. For the non-prompt J/ψ, the R_{AA} shows a slightly increasing suppression towards central collisions and higher p_{T}, and is described by theoretical models implementing heavy quark energy loss mechanisms inside the medium.

REFERENCES

[1] H. Satz, *Nucl. Phys. A* **783**, 249 (2007), arXiv:hep-ph/0609197.

[2] P. Braun-Munzinger, J. Stachel, *Phys. Lett. B* **490**, 196 (2000).

[3] A. Andronic *et al.*, *Phys. Lett. B* **797**, 134836 (2019), arXiv:1901.09200 [hep-th].

[4] K. Zhou *et al.*, *Phys. Rev. C* **89**, 054911 (2014), arXiv:1401.5845 [nucl-th].

[5] X. Du, R. Rapp, *Nucl. Phys. A* **943**, 147 (2015), arXiv:1504.00670 [hep-ph].

[6] R.L. Thews *et al.*, *Phys. Rev. C* **63**, 054905 (2001), arXiv:hep-ph/0007323.

[7] N. Armesto *et al.*, *Phys. Rev. D* **69**, 114003 (2004), arXiv:hep-ph/0312106.

[8] A. Adil, I. Vitev, *Phys. Lett. B* **649**, 139 (2007), arXiv:hep-ph/0611109.

[9] ALICE Collaboration, *Nature* **605**, 440 (2022), arXiv:2106.05713 [nucl-ex].

[10] ALICE Collaboration, *J. High Energy Phys.* **221**, 174 (2022), arXiv:2110.09420 [nucl-ex].

[11] ALICE Collaboration, *J. Instrum.* **3**, S08002 (2008).

[12] CMS Collaboration, *Eur. Phys. J. C* **78**, 509 (2018), arXiv:1712.08959 [nucl-ex].

[13] ATLAS Collaboration, *Eur. Phys. J. C* **78**, 762 (2018), arXiv:1805.04077 [nucl-ex].

[14] ALICE Collaboration, arXiv:2202.00815 [nucl-ex].

[15] A. Andronic *et al.*, *J. High Energy Phys.* **2107**, 035 (2021), arXiv:2104.12754 [hep-ph].

[16] S. Aronson *et al.*, *Phys. Lett. B* **778**, 384 (2018), arXiv:1709.02372 [hep-ph].

[17] Y. Makris, I. Vitev, *J. High Energy Phys.* **1910**, 111 (2019), arXiv:1906.04186 [hep-ph].

[18] S. Shi *et al.*, *Chinese Phys. C* **43**, 044101 (2019), arXiv:1808.05461 [hep-ph].

[19] S. Shi *et al.*, *Chinese Phys. C* **42**, 104104 (2018), arXiv:1804.01915 [hep-ph].

[20] D. Zigic *et al.*, arXiv:2110.01544 [nucl-th].

[21] S. Stojku *et al.*, *Phys. Rev. C* **105**, L021901 (2022), arXiv:2008.08987 [nucl-th].

[22] ALICE Collaboration, ALICE-PUBLIC-2018-011, 2018.

[23] NA50 Collaboration, *Eur. Phys. J. C* **49**, 559 (2007), arXiv:nucl-ex/0612013.